Roughness distributions for $1/f^{\alpha}$ signals

T. Antal,[1,2,*] M. Droz,[1,†] G. Györgyi,[2,‡] and Z. Rácz[2,3,§]
[1]*Département de Physique Théorique, Université de Genève, CH 1211 Genève 4, Switzerland*
[2]*Institute for Theoretical Physics, Eötvös University, 1117 Budapest, Pázmány sétány 1/a, Hungary*
[3]*Laboratoire de Physique Théorique, Bâtiment 210, Université de Paris-Sud, 91405 Orsay Cedex, France*
(Received 15 December 2001; published 10 April 2002)

The probability density function (PDF) of the roughness, i.e., of the temporal variance, of $1/f^{\alpha}$ noise signals is studied. Our starting point is the generalization of the model of Gaussian, time periodic, $1/f$ noise, discussed in our recent Letter [Phys. Rev. Lett. **87**, 240601 (2001)], to arbitrary power law. We investigate three main scaling regions ($\alpha \leqslant 1/2$, $1/2 < \alpha \leqslant 1$, and $1 < \alpha$), distinguished by the scaling of the cumulants in terms of the microscopic scale and the total length of the period. Various analytical representations of the PDF allow for a precise numerical evaluation of the scaling function of the PDF for any α. A simulation of the periodic process makes it possible to study also nonperiodic, thus experimentally more relevant, signals on relatively short intervals embedded in the full period. We find that for $\alpha \leqslant 1/2$ the scaled PDFs in both the periodic and the nonperiodic cases are Gaussian, but for $\alpha > 1/2$ they differ from the Gaussian and from each other. Both deviations increase with growing α. That conclusion, based on numerics, is reinforced by analytic results for $\alpha = 2$ and $\alpha \to \infty$, in the latter limit the scaling function of the PDF being finite for periodic signals, but developing a singularity for the aperiodic ones. Finally, an overview is given for the scaling of cumulants of the roughness and the various scaling regions in arbitrary dimensions. We suggest that our theoretical and numerical results open a different perspective on the data analysis of $1/f^{\alpha}$ processes.

DOI: 10.1103/PhysRevE.65.046140 PACS number(s): 05.70.Ln, 64.60.Cn, 82.20.−w

I. INTRODUCTION

The power spectra of fluctuations scale with frequency as $S(f) \sim 1/f^{\alpha}$ in a large variety of physical, chemical, and biological systems [2]. This power-law behavior $1/f^{\alpha}$ often persists over several orders of magnitude with cutoffs present at both high and low frequencies, and with typical values of α in the range $0.8 \leqslant \alpha \leqslant 4$ [2]. In a somewhat loose terminology, all these systems are said to display $1/f$ noise although good quality data with α very close to 1 exist only for the voltage fluctuations when a current is flowing through a resistor [3,4]. Phenomena with $\alpha \neq 1$, however, are abundant, examples being the white-dwarf light emission [5], the flow of sand through an hourglass [6], ionic current fluctuations in membrane channels [7], the number of daily trades in the stock market [8], water flows of rivers [9], the spike trains of nerve cells [10], the occurrence of earthquakes [11], the traffic flow on a highway [12,13], the electric noise in carbon nanotubes [14] and in nanoparticle films [15], the interface fluctuations [16], and dissipation in turbulent systems [17]. The list could be continued.

A well-understood example of $1/f^{\alpha}$ type behavior is the dynamic scaling observed at equilibrium critical points where the power-law correlations in time are generated by the infinite-range correlations in space. Most of the examples listed above, however, are related to nonequilibrium phenomena and a similar level of understanding does not exist. There have been many attempts at identifying possible generic mechanisms leading to scale invariant fluctuations, a notable example being the concept of self-organized criticality [18,19]. It is clear, however, that not all the systems showing a $1/f^{\alpha}$ noise fit into a single scheme and, perhaps, at this stage one should pursue a less ambitious aim of developing more detailed characterizations of nonequilibrium universality classes.

In equilibrium systems, the static universality classes are determined by the (i) dimensionality, (ii) symmetry of the order parameter, and (iii) the range of the interactions. Further specifying the conservation laws and the coupling of the order parameter to conserved quantities defines then the dynamical universality classes. The statics and dynamics are, however, intertwined in nonequilibrium systems and an exponent in the $1/f^{\alpha}$ behavior carries information about both. Thus, measuring a single exponent α (a characteristic situation when measuring time series of noise) does not determine the universality class of the system even within the framework of an equilibrium-type theory. Having a single exponent, however, one can still go on and try to ascertain whether or not two systems belong to the same universality class. This can be done by using the data to measure and compare the scaling functions associated with the finite-size scaling of some global physical quantity such as, e.g., the order parameter in a critical system or the roughness of an interface.

The remarkable features of scaling functions are that they are obtained without any fitting procedure and, furthermore, they usually converge fast as the system size is increased. Thus one can build a picture gallery that can be effectively used to identify systems belonging to a given universality class. Indeed, such an approach has been useful in establishing connections among rather diverse processes such as massively parallel algorithms [20], interface dynamics in the

*Electronic address: Tibor.Antal@physics.unige.ch
†Electronic address: Michel.Droz@physics.unige.ch
‡Electronic address: gyorgyi@glu.elte.hu
§Electronic address: racz@poe.elte.hu

$d=2$ Fisher-Kolmogorov equation [21], dissipation fluctuations in a turbulence experiment [22,23], and the interface fluctuations in the $d=2$ Edwards-Wilkinson model, which is equivalent to the XY model treated in [24,25]. This scaling function approach has also helped to clear up some questions about the upper critical dimension of the Kardar-Parisi-Zhang equation [26].

In our attempts to expand the picture gallery, we have recently derived [1] the following result: The scaling function for the roughness distribution of a Gaussian periodic $1/f$ noise signal is one of the extreme value distributions, the Fisher-Tippet-Gumbel distribution [27,28]. This is a rather unexpected and interesting result and we feel that it is important to explore its generality and limitations. First, because ideas about extreme statistics playing a role in strongly correlated, scale-invariant systems have been much discussed [29–31,45,46], and this result may provide a foundation to those speculations. Second, because this is the first instance when one of the distributions associated with extreme statistics emerges naturally, and in a mathematically precise manner, for a quantity which is not of extremal character *a priori*.

There are three elements underlying the above extreme statistics results: Gaussianity, $1/f$ power spectrum, and periodicity. Thus the problem can be generalized by considering effects of (1) non-Gaussianity, (2) a generalized power spectra of the form $1/f^{\alpha}$, and (3) nonperiodicity (the experimentally realistic situation). In this paper, we shall concentrate on points (2) and (3) leaving the more difficult problem of non-gaussianity to a later study.

One expects that changing the exponent α will change the roughness distribution of a signal and, indeed, there are analytical results [1,32,33] for $\alpha=1,2,4$ which demonstrate this explicitly for periodic signals ($d=1$ dimensional systems). Similar results exist also for higher dimensions where the roughness of a $d=1$ signal is replaced by the roughness of a higher-dimensional interface [24,25,34,35]. Thus the questions we address in connection with the α dependence is not about its existence but about its magnitude (observability). More specifically, we ask if there is an interval of α where the α dependence is absent or negligible from an experimental point of view?

The other problem of our concern is the question of the effect of the boundary conditions (BCs). When analyzing a signal and building a distribution function, one usually divides the signal into equal ''time'' intervals and measures the quantity of interest in every interval. Thus the signal within a given interval is not periodic (usually the total signal is not periodic either) and the question arises whether the experimentally used BC, i.e., when one studies a ''window'' within the signal, would affect the scaling functions or not. This shall be a central issue in this paper, so we introduce the abbreviations PBC and WBC, for periodic and ''window'' BC, respectively.

The dependence of scaling functions on the boundary conditions has been discussed in equilibrium critical phenomena and it is known that such dependence exist [36,37]. Thus our aim here again is not to show its presence but to gauge its magnitude for various α values and investigate for which values of α this effect is absent or negligible.

As we show below, the scaling functions can be derived analytically in the case of PBC. Similar analytical treatment for WBC were achieved only for $\alpha=2$ and in the $\alpha\to\infty$ limit, otherwise we had to resort to simulations in order to obtain the finite alpha results. Observing the scaling functions (displayed on the figures below) one can deduce the following qualitative trends as α is decreased:

(1) The PBC scaling functions change smoothly apart from $\alpha\approx 1$ where the function is sensitive to small changes in α since a singularity develops at $\alpha=1$. Even this singular behavior can be smoothed out, however, by an appropriate change of the scaling variable. The scaling function approaches a Gaussian as $\alpha\to 1/2$ and it remains a Gaussian for $\alpha<1/2$.

(2) The WBC scaling functions display strong α dependence at large α. The dependence becomes weaker for $\alpha \lesssim 2$ and, similarly to the PBC case, the α dependence disappears entirely for $\alpha\leqslant 1/2$ where the function becomes a Gaussian.

(3) Comparing the PBC and WBC scaling functions, one can observe that their difference is large for $\alpha\gtrsim 4$, it is easily noticeable in the range between 1 and 4, while it becomes harder to distinguish the functions for $\alpha\lesssim 1$, and the functions become identical Gaussians for $\alpha\leqslant 1/2$.

In order to demonstrate the above observations, we shall introduce a model of $1/f^{\alpha}$ noise in Sec. II where the roughness distribution, the appropriate choice of scaling variables, and some general scaling properties will also be discussed. Section III contains the analytical calculations for the case of PBC while Sec. IV is devoted to presenting both the simulation and analytical results for the WBC case. We close with discussing generalizations to higher dimensions in Sec. V.

II. PROBABILITY DISTRIBUTION OF PERIODIC $1/f^{\alpha}$ SIGNALS AND THEIR ROUGHNESS

A. Model for periodic, perfectly $1/f^{\alpha}$, Gaussian noise

Noisy signals are in principle fully characterized by their path probability density functional. However, the most often used characterization is by the power spectrum, whose experimental recording is straightforward. This leaves several properties unspecified, such as the distribution of the phases, and whether the noise is Gaussian. Furthermore, the usual Fourier expansion of the signal in an interval implies periodicity outside the interval. While that expansion can be used well for data analysis, the physical implication for the outer part of the signal, which influences by long-time correlations the inner part, is obviously nonrealistic. Accordingly, the role of initial and final conditions in time, a property that we shall call boundary condition (BC), are generically neglected. Whereas it is arguable that in a stationary process, a long time after the turning on of the experimental device, the boundary conditions should not have much influence, when a model is constructed for $1/f^{\alpha}$ noise, the boundary conditions should be defined with care.

We now describe the main properties of the model treated in this paper. It should be emphasized that we do not study the underlying microscopic mechanism that may lead to $1/f^{\alpha}$

noise, this has been done on many different levels of simplification for a large number of systems, for a review see [3]. Rather, we construct a stochastic model, where the noisy signal is given by its path probability density functional, having the generic properties of observed $1/f^{\alpha}$ noises. In a sense it will be a minimal model tailored to exhibit a few properties we prescribe.

First, the noise we consider is periodic. While this is obviously not valid in a real experimental situation over the time interval of the measurement, as we have seen recently [1], it yields theoretical predictions not very far from what is measured in a real signal. Furthermore, the periodic boundary condition (PBC) allows for the straightforward numerical simulation of the noise, thus making it possible to study numerically the statistics in cut-out time intervals that are much smaller than the entire period. Such a ''window'' boundary condition (WBC) is, we surmise, a more faithful representation of experimentally realistic BCs. Indeed, while the effect of the outer signal onto the inner part is important due to long-time correlations, probably it depends little on whether the signal was simply turned on a long time ago, or is periodic on a time scale much larger than the ''window.'' Looking at it from another angle we can say that the PBC is equivalent to saying that the signal is best expanded in the usual Fourier basis, thus what remains is to specify the probability distribution of the Fourier coefficients. Note that the noisy signal in a ''window'' should not be expanded in such a basis in theory, because the noise is manifestly aperiodic.

Second, we restrict ourself to Gaussian noise and assume that the Fourier modes are independent random variables. The reasons for this working hypothesis are that many experimental data concern power spectrum measurements of Gaussian noises and provide no information about the coupling between the modes.

Third, we assume that the phase of each complex Fourier component is random and uniformly distributed in $[0,2\pi]$. Hence, the probability distribution will depend only on the modulus.

Last but not least, we consider perfectly $1/f^{\alpha}$ noise. Here we understand that the variance of the independent Fourier amplitudes of a path is a pure power with exponent α. Furthermore, there are no upper- and lower-cutoff frequencies other than the natural ones determined by the observation time and the microscopic characteristic time unit, respectively.

The above ingredients specify the path probability of the stochastic time signal, this will be our model, as discussed in detail below. (Note that it is a generalization of the case $\alpha=1$ [1] to arbitrary α.)

The stochastic trajectories $h(t)$ are periodic, $h(t)=h(t+T)$, thus the trajectory can be expanded as

$$h(t)=\sum_{n=-N}^{N} c_n e^{2\pi i n t/T}, \quad c_n^*=c_{-n}. \tag{1}$$

Here we have used a cutoff N meaning that the time scale is not resolved below $\tau=T/N$. This is needed to deal with some singularities and may have microscopic physical origin. Whenever possible we shall, however, take $N\to\infty$, and even if this were a singular limit, we shall wind up with scaling functions not containing the microscopic time unit, so the value of τ may be left undetermined.

The stochastic properties of a signal $h(t)$ are fully characterized by our specifying the probability density functional

$$P[h(t)]=e^{-S[h(t)]}, \tag{2}$$

or, equivalently, the probability density function (PDF) for the Fourier coefficients c_n for $n=0\ldots N$ as

$$P(\{c_n\})=A\,e^{-S(\{c_n\})}. \tag{3}$$

Our model for periodic, perfectly $1/f^{\alpha}$ signals is defined by the action

$$S(\{c_n\})=2\sigma T^{1-\alpha}\sum_{n=1}^{N} n^{\alpha}|c_n|^2, \tag{4}$$

$$A=\prod_{n=1}^{N} 2\sigma n^{\alpha} T^{1-\alpha}\pi^{-1}, \tag{5}$$

where the probabilistic variables are the real and imaginary parts of c_n-s.[1] We assume translation invariance in h space, therefore the action must not depend on the constant part c_0 and we set that to zero hereafter. Note furthermore that the above action means that different Fourier modes are uncorrelated. The coefficient σ makes S dimensionless and can be understood as the reciprocal noise intensity parameter. Since we are after scaling functions, the value of σ will not matter. The above action was set up so that the power spectrum is

$$\langle|c_n|^2\rangle\propto\frac{1}{n^{\alpha}}, \tag{6}$$

thus the process is indeed of the $1/f^{\alpha}$-type.

B. Roughness of a signal

Our aim is to characterize the signals by some global properties. As the time average c_0 in Eq. (1) was set to zero, the simplest quantity worth considering is the mean-square width, i.e., roughness of the signal. This has been studied for the $1/f$ noise ($\alpha=1$) in Ref. [1], the Wiener process ($\alpha=2$) in Ref. [32], and for curvature-driven interfaces ($\alpha=4$) in Ref. [33]. Its general definition is

$$w_2=\overline{[h(t)-\overline{h(t)}]^2}=\overline{h^2(t)}-\overline{h(t)}^2, \tag{8}$$

[1]In time representation the action is of the form

$$S[h(t)]=2\sigma\left(\frac{-1}{2\pi}\right)^{\alpha}\int_0^T dt\left(\frac{d^{\alpha/2}h}{dt^{\alpha/2}}\right)^2, \tag{7}$$

where the fractional derivative is understood on the Fourier representation so that it acts upon the phase factor as $d^{\beta}e^{iat}/dt^{\beta}=(ia)^{\beta}e^{iat}$. Dimensional analysis on Eq. (7) yields the scaling by T used in Eq. (4).

where overbar means time average over the entire period T. Note that now $\overline{h(t)}=0$. In Fourier representation we get

$$w_2=2\sum_{n=1}^{N}|c_n|^2, \tag{9}$$

hence w_2 is in fact the integrated power spectrum.

The roughness w_2 is associated with a given $h(t)$ trajectory, it varies when different instances of the paths are taken from their ensemble. Thus, w_2 is a probabilistic variable, whose PDF can be expressed as

$$P(w_2)=\int \delta(w_2-\overline{h^2(t)}+\overline{h(t)}^2)P[h(t)]\mathcal{D}h(t). \tag{10}$$

In the more practical Fourier representation $P(w_2)$ assumes the form

$$P(w_2)=\int \delta\left(w_2-2\sum_{n=1}^{N}|c_n|^2\right)P(\{c_n\}) \times\prod_{n=1}^{N} d\,\mathrm{Re}\,c_n\, d\,\mathrm{Im}\,c_n. \tag{11}$$

It is useful to introduce the generating function of the moments of $P(w_2)$ as

$$G(s)=\int_0^\infty dw_2 P(w_2)e^{-sw_2}, \tag{12}$$

which by Eq. (11) gives

$$G(s)=\prod_{n=1}^{N}\left(1+\frac{s}{\sigma T^{1-\alpha}n^\alpha}\right)^{-1}. \tag{13}$$

The cumulant generating function $\Psi(s)$ can be obtained by expanding the logarithm as

$$\Psi(s)=\ln G(s)=\sum_{k=1}^{\infty}\frac{1}{k}\left(\frac{-s}{\sigma T^{1-\alpha}}\right)^k\sum_{n=1}^{N}\frac{1}{n^{\alpha k}}. \tag{14}$$

Hence the kth cumulant of the roughness is

$$\kappa_k=\frac{(k-1)!}{(\sigma T^{1-\alpha})^k}\sum_{n=1}^{N}\frac{1}{n^{\alpha k}}. \tag{15}$$

Note that for $\alpha k>1$ the cumulants can be expressed in terms of Riemann's zeta function in the limit of large N as

$$\kappa_k\to\frac{(k-1)!}{(\sigma T^{1-\alpha})^k}\zeta(\alpha k). \tag{16}$$

The low-order cumulants have the usual meaning of average and variance

$$\kappa_1=\langle w_2\rangle=\frac{1}{\sigma T^{1-\alpha}}\sum_{n=1}^{N}\frac{1}{n^\alpha}, \tag{17a}$$

$$\kappa_2=\langle w_2^2\rangle-\langle w_2\rangle^2=\frac{1}{(\sigma T^{1-\alpha})^2}\sum_{n=1}^{N}\frac{1}{n^{2\alpha}}. \tag{17b}$$

The PDF corresponding to the generator (13) will be the main concern of this paper. We shall also discuss the "window" boundary condition, WBC, so in case of ambiguity the above quantities, pertaining to PBC, will get a subscript like $G_{\mathrm{p}}(s)$.

C. Scaling of averages

The generating function of the PDF of the roughness still contains two scales, the observation time T (multiplied by $\sigma^{1/(1-\alpha)}$) and the microscopic time unit $\tau=T/N$. If N diverges, physical quantities will exhibit various scaling for different α-s. Whereas the above model is a very simple one from the viewpoint of the statistical mechanics of critical phenomena, as it is Gaussian and massless, it is worth summarizing the scaling properties of averaged quantities, because they contain important information about the PDF.

The kth roots of the kth cumulants (15) for all k-s have the dimensionality of the roughness, however, their scaling in the length T of the time interval may be different. For $k=1,2$ these are the average and the mean deviation there from, respectively. First, for $\alpha>1$ all cumulants converge in the limit $N\to\infty$ and we have

$$\sqrt[k]{\kappa_k}\propto T^{\alpha-1}. \tag{18}$$

If $\alpha=1$ then the average, κ_1, logarithmically diverges in $N=T/\tau$ while all higher cumulants remain of unit order, independent of T and τ. This corresponds to a critical dimension in second-order phase transitions, but here we have a critical $\alpha=1$ where the logarithmic singularity occurs. For $\alpha<1$ the average no longer depends on T, rather it is proportional to $\tau^{1-\alpha}$, and for $1/2<\alpha<1$ the $k>1$ cumulants still exhibit the scaling (18). The second critical value of α is at 1/2, where the second cumulant has a logarithmic singularity. For $\alpha<1/2$ the $\sqrt[2]{\kappa_2}$ becomes proportional to $T^{-1/2}\tau^{\alpha-1/2}$, while higher-than-second order cumulants still satisfy Eq. (18) until the third critical value of $\alpha=1/3$ is reached. Continuing the reasoning shows that at $\alpha_k=1/k$ the kth-order cumulant develops a logarithmic singularity. A significant change occurs at $\alpha_2=1/2$, because for lesser α-s the scale of the mean deviation ($k=2$) will dominate over the scale from higher k-s. This means that the PDF of the roughness on the scale of its mean deviation becomes Gaussian in the $N\to\infty$ limit. Thereby the effect of the sequence of critical α_k-s for $k>2$ is suppressed. Table I summarizes the scaling of the cumulants. Note that the powers of T and τ add up to $\alpha-1$ for each entry to produce the right time dimensionality.

As mentioned above and can be seen in Table I, for $\alpha<1/2$ the mean deviation goes with the $-1/2$-th power of the size T. This result would follow if the central limit theorem could be applied to the roughness as given in Eq. (9). This is analogous to the mean-field behavior beyond the upper critical dimension of a statistical mechanical system exhibiting a second-order phase transition.

TABLE I. Scaling of the cumulants for various α-s. The dots indicate that the last formula is valid from then on, i.e., " . . . " extends the validity to higher k-s and vertical dots to lower α-s.

Range or value of α	κ_1	$\sqrt{\kappa_2}$	$\sqrt[3]{\kappa_3}$	$\sqrt[4]{\kappa_4}$	
$(1,\infty)$	$T^{\alpha-1}$	$\cdots$			
1	$\ln\frac{T}{\tau}$	O(1)	$\cdots$		
(1/2,1)	$\tau^{\alpha-1}$	$T^{\alpha-1}$	$\cdots$		
1/2	$\vdots$	$T^{-1/2}\sqrt{\ln\frac{T}{\tau}}$	$T^{-1/2}$	$\cdots$	
(1/3,1/2)		$\tau^{\alpha-1/2}\ T^{-1/2}$	$T^{\alpha-1}$	$\cdots$	
1/3		$\vdots$	$T^{-2/3}\sqrt[3]{\ln\frac{T}{\tau}}$	$T^{-2/3}$	$\cdots$
(1/4,1/3)			$\tau^{\alpha-1/3}\ T^{-2/3}$ $\vdots$	$T^{\alpha-1}$	$\cdots$

Since the $\alpha=1$ value is a threshold in the sense that for $\alpha>1$, the scales of all cumulants diverge as $T^{\alpha-1}$, while for $\alpha<1$ the average becomes independent of T and higher cumulants vanish, the natural scaling for the two cases is different. If $\alpha>1$ the scaled quantity

$$x=\frac{w_2}{\kappa_1} \tag{19}$$

has, in the limit $N\to\infty$, a convergent PDF, devoid of any adjustable parameter. In the following, we shall refer to the use of variable x as scaling by the average. For $\alpha\leqslant 1$ the same PDF would be a Dirac delta centered on one, so one rather resorts to a scaling that effectively widens the delta peak. One can do that by introducing [24,25]

$$y=\frac{w_2-\kappa_1}{\sqrt{\kappa_2}}, \tag{20}$$

that is, scaling the roughness by the variance. The PDF as a function of y will clearly become Gaussian below $\alpha=1/2$, but develop a nontrivial shape for $1/2<\alpha$. This variable was used in our recent Letter on the $\alpha=1$ case [1], where we used the notation x for it. We will adopt the notation that functions of x and y carry the labels 1 and 2, respectively. So, e.g., the PDF of the scaled quantity (19) will be denoted by $\Phi_1(x)$.

The two scalings (19) and (20) can lead to dramatically different shapes. For instance, for $\alpha\to 1$ from above, Eq. (19) yields a peak centered at $x=1$ and leads to a Dirac delta at $x=1$ for $\alpha<1$. However, Eq. (20) gives smooth functions continuously changing when α passes through one and accordingly, we will use sometimes Eq. (20) in the region $\alpha>1$ for the sake of comparison.

III. SCALING FUNCTION FOR PERIODIC BOUNDARY CONDITION

A. Analytic approach for general α

Knowing the explicit form of the generating function (13), the roughness distribution for any finite N can be obtained by inverting the Laplace transformation (12)

$$P_{\rm p}(\alpha,w_2,T)=\int_{-i\infty}^{i\infty}\frac{ds}{2\pi i}e^{w_2 s}\prod_{n=1}^{N}\left(1+\frac{s}{\sigma T^{1-\alpha}n^{\alpha}}\right). \tag{21}$$

From here we concentrate on the $N\to\infty$ limit. In this limit the PDF of the scaling variable x or y, defined in Eqs. (19) and (20), becomes independent of T. Scaling by the variance, that is, using the y variable of Eq. (20), has the advantage to yield smooth PDFs for all α-s. We refer to this type of scaling by the label 2 on the PDF. For $\alpha>1/2$ that PDF is

$$\begin{aligned}\Phi_{2{\rm p}}(\alpha,y)&=\sqrt{\kappa_2}P_{\rm p}(\alpha,w_2,T)\\&=\sqrt{\zeta(2\alpha)}\int_{-i\infty}^{i\infty}\frac{ds}{2\pi i}e^{\sqrt{\zeta(2\alpha)}ys}\prod_{n=1}^{\infty}\frac{e^{s/n^{\alpha}}}{1+\frac{s}{n^{\alpha}}}.\end{aligned} \tag{22}$$

The integrand has simple poles along the real axes and their contributions can be easily collected

$$\Phi_{2{\rm p}}(\alpha,y)=\sqrt{\zeta(2\alpha)}\sum_{m=1}^{\infty}m^{\alpha}e^{-m^{\alpha}\sqrt{\zeta(2\alpha)}y-1}Y_2(\alpha,m), \tag{23}$$

where

$$Y_2(\alpha,m)=\prod_{n=1,\neq m}^{\infty}\frac{e^{-(m/n)^{\alpha}}}{1-\left(\frac{m}{n}\right)^{\alpha}}. \tag{24}$$

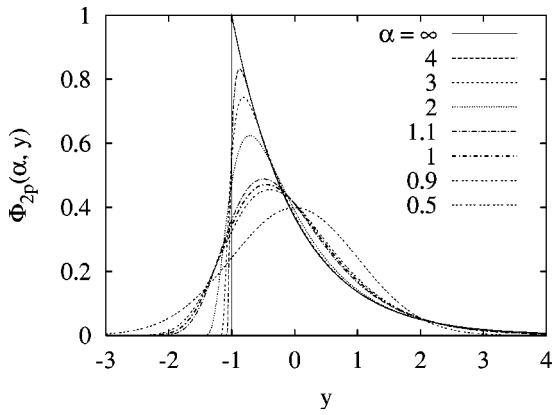

FIG. 1. Roughness distribution of periodic signals, Eq. (23), for different values of α as a function of the scaling variable (20). Note that the PDF is a smooth function of α for all α-s.

This series can be considered as the large-y expansion of the PDF. It is a general formula for any $\alpha > 1/2$ and can be evaluated numerically. First, the precise numerical values of $Y_2(\alpha,m)$ should be determined up to a certain $m_{\max}$. Greater $m_{\max}$ is needed for smaller values of y. Since the sign of $Y_2(\alpha,m)$ is known to be $(-1)^{m-1}$, it suffices to evaluate $|Y_2|$. The logarithm of $|Y_2|$ can be written as an infinite sum, which can be tackled numerically. Once the values of $Y_2(\alpha,m)$ are given, the summation in Eq. (23) can be done easily due to the exponential cutoff in m. The resulting PDF is depicted on Figs. 1 and 2 for several values of α. On the Fig. 2 logarithmic scale was used for the ordinate to make the tails visible for several decades. It is clearly seen on these figures that the shape of the PDF depends smoothly on the value of α.

When $\alpha > 1$, the natural choice for scaling variable is x of Eq. (19), and the PDF in terms of x can be obtained by changing the variable in Eq. (23) and making some simplifications

$$\Phi_{1p}(\alpha,x) = \kappa_1 \Phi_p(\alpha, w_2, T) = \zeta(\alpha) \sum_{m=1}^{\infty} m^{\alpha} e^{-x m^{\alpha} \zeta(\alpha)} Y_1(\alpha,m) \qquad (25)$$

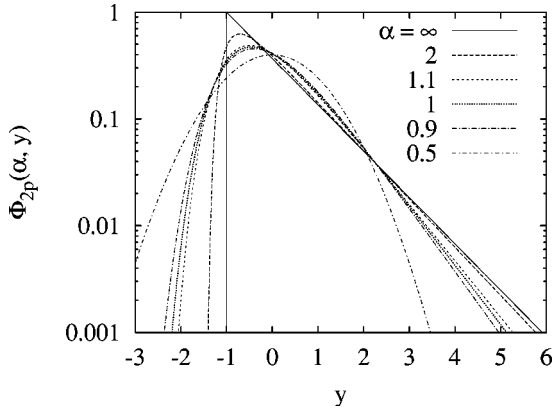

FIG. 2. The same as Fig. 1 but on log-linear scale.

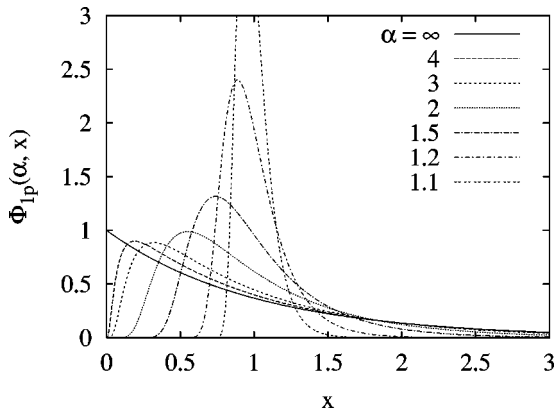

FIG. 3. Roughness distribution of periodic signals for different values of α as a function of the scaling variable (19). Note that as $\alpha \to 1$ the PDF dramatically sharpens and converges to a Dirac delta function centered at $x = 1$.

with

$$Y_1(\alpha,m) = \prod_{n=1,\neq m}^{\infty} \left[1 - \left(\frac{m}{n} \right)^{\alpha} \right]^{-1}. \qquad (26)$$

Note that it is more appropriate for numerical evaluation to use Eqs. (23) and (24) and then change the variable y to x. The PDFs on Fig. 3 were calculated this way. One can observe the singularity at $x = 1$ emerging as α approaches 1.

For integer values of $\alpha > 1$ the infinite product (26) can be written in a closed form

$$Y_1(\alpha,m) = \frac{m!(-1)^{m-1}}{\alpha} \prod_{k=1}^{\alpha-1} \Gamma(1 - a^k m), \qquad (27)$$

where $a = \exp(2\pi i/\alpha)$. For $\alpha = 2$ we recover the random walk result of Ref. [32]

$$Y_1(2,m) = 2(-1)^{m-1}. \qquad (28)$$

In the $\alpha = 4$ case there are three factors in the product and using some basic properties of the Γ function one obtains

$$Y_1(4,m) = \frac{4\pi m(-1)^{m-1}}{\sinh(\pi m)}, \qquad (29)$$

a result which agrees with that of Ref. [33].

Using Eq. (27), we can write the roughness distribution for any integer $\alpha > 1$ in the relatively simple form

$$\Phi_{1p}(\alpha,x) = \alpha \zeta(\alpha) \sum_{m=1}^{\infty} \frac{(-1)^{m-1} m^{\alpha}}{m!} \times e^{-m^{\alpha} \zeta(\alpha) x} \prod_{k=1}^{\alpha-1} \Gamma(1 - a^k m). \qquad (30)$$

The curves for PBC in all figures with integer $\alpha > 1$ were drawn based on this formula.

B. Special cases

1. 1/f noise ($\alpha=1$)

Here we briefly revisit the case of $1/f$ noise presented in our recent Letter [1]. The natural scaling goes now by the variance as in Eq. (20). From Eq. (22) the generator of the scaling function $\Phi_{2p}(1,y)$ is

$$G_{2p}(1,s)=\prod_{n=1}^{\infty}\frac{e^{s/an}}{1+\frac{s}{an}}, \tag{31}$$

where the upper limit of the product could safely be taken to infinity and $a=\pi/\sqrt{6}$. This formula produces the gamma function as

$$G_{2p}(1,s)=e^{\gamma s/a}\Gamma\left(1+\frac{s}{a}\right)=\int_0^{\infty}du\,e^{-u}(u\,e^{\gamma})^{s/a}, \tag{32}$$

where γ is Euler's constant and we also displayed Euler's integral formula for the gamma function [38]. Introducing the variable $y=-(\ln u+\gamma)/a$ we finally get

$$G_{2p}(1,s)=\int_{-\infty}^{\infty}dy\,e^{-sy}\Phi_{2p}(1,y), \tag{33a}$$

$$\Phi_{2p}(1,y)=a\,e^{-(ay+\gamma)-e^{-(ay+\gamma)}}. \tag{33b}$$

The inverse Laplace transformation on Eq. (33a) gives Eq. (33b), so $\Phi_{2p}(1,y)$ is the sought PDF of the roughness scaled by the variance. Note that strictly speaking Eq. (33a) is not a Laplace transformation anymore, due to the shift of the average of $\Phi_{2p}(1,y)$ to zero, but the inverse transformation can still be performed. In such cases the Fourier transformation is better suited for the generating function, because the variable y of Eq. (20) is not restricted to nonnegative numbers, but we could still derive the scaling function (33b) within the Laplace formalism.

The formula (33b) is a special case of what is known as the Fisher-Tippet-Gumbel function that emerges in extreme value statistics [27,28]. This comes about in a nutshell as follows. Suppose we have a random variable with some generic PDF, and we draw M times independently from this distribution. The PDF of the kth largest of all those values, that is, the extreme value PDF, will be centered around a median increasing with M. Obviously, for $M\to\infty$ and k fixed, the extreme value PDF will be determined by the tail of the original PDF. In this limit, an appropriate linear rescaling of the kth largest value yields generally an M-independent scaling function for the extreme value PDF. Now, in practical terms, if the original PDF has a tail decaying faster than any power law, then the scaling function is the Fisher-Tippet-Gumbel distribution. Our scaling function (33b) corresponds to the $k=1$ case, scaled to have zero average and unit variance.

The fact that Eq. (33b) is related to extremal value statistics does not reveal automatically the mechanism of selection of extremes in the case of the roughness of a signal. Also, it should be emphasized that we do not have the usual extremal value distribution functions for α-s other than one. So our result raises the problems of why the $1/f$ noise is distinguished among all α-s and how extreme value selection comes about there rather than resolves them.

2. Wiener process ($\alpha=2$)

For the Wiener process with PBC the generating function as well as the asymptotics of the PDF for small and large x has been derived in [32]. Interestingly, the distribution can be expressed in terms of a known function. The normalization (19), natural for $\alpha>1$, will be used. For the integrated density with $\alpha=2$ we get from Eq. (25)

$$M_{1p}(2,x)=\int_0^x\Phi_{1p}(2,\overline{x})d\overline{x}=1+2\sum_{k=1}^{\infty}(-1)^k e^{-\pi^2k^2x/6}$$
$$=\vartheta_4(0,e^{-\pi^2x/6}). \tag{34}$$

ϑ_4 is Jacobi's fourth theta function [38] and its second argument is now the relevant variable [39].

The PDF can also be written in a closed, implicit form in terms of complete elliptic integrals of the first and second kind [$K(k)$ and $E(k)$]

$$\Phi_{1p}[2,x(k)]=\frac{1}{3\sqrt{2\pi}}(1-k^2)^{1/4}K^{3/2}(k)[K(k)-E(k)], \tag{35a}$$

$$x(k)=\frac{6K(\sqrt{1-k^2})}{\pi K(k)}. \tag{35b}$$

The sum over poles described in Sec. III A for a general α can be understood as the large-x expansion of the distribution. On the other hand, we also have a small-x series for the special $\alpha=2$ case. This can be constructed by scaling the generating function (13) according to Eq. (19), expanding it as

$$G_{1p}(2,s)=\frac{\sqrt{6s}}{\sinh\sqrt{6s}}=2\sqrt{6s}\sum_{k=0}^{\infty}e^{-(2k+1)\sqrt{6s}}, \tag{36}$$

and using the inverse Laplace transform

$$\int_{c-i\infty}^{c+i\infty}\frac{ds}{2\pi i}e^{sx}\sqrt{s}\,e^{-a\sqrt{s}}=\frac{a^2-2x}{4\sqrt{\pi x^5}}e^{-a^2/4x}. \tag{37}$$

The result is

$$\Phi_{1p}(2,x)=\int_{c-i\infty}^{c+i\infty}\frac{ds}{2\pi i}e^{sx}G_{1p}(2,s)$$
$$=\sqrt{\frac{6}{\pi x^5}}\sum_{k=0}^{\infty}[3(2k+1)^2-x]e^{-3(2k+1)^2/2x}. \tag{38}$$

One recovers here the nonanalytic small-x asymptotics shown in [32], and one also has the corrections to it. Three

terms from the sum suffice to produce the PDF $\Phi_{1p}(2,x)$ with a uniform error bound of $\epsilon = 4 \times 10^{-5}$ in the sense that either the approximation is within ϵ from the PDF, or the PDF is less than ϵ. The precision of this approximation is, however, much better when the PDF is of order unity. To give a feeling of that, one gets 29 digits of the PDF at $x = 1$. The series can be considered as the small-x expansion of the derivative of the theta function (34), not available in [38]. The formulas of Secs. III B 1 and III B 2 can help to test the numerical evaluation of the series (23)–(26).

3. Large α limit

For large α the lowest-frequency mode dominates. Indeed, in the action (4) the coefficients c_n with $n>1$ will have very small variance compared to the $n=1$ case, so practically they are zero. The corresponding generator function is obtained from Eq. (13) by omitting all $n>1$ factors. Applying the scaling (19) we get

$$G_{1p}(\infty,s) = (1+s)^{-1}, \tag{39}$$

whence inverse Laplace transformation yields

$$\Phi_{1p}(\infty,x) = e^{-x}. \tag{40}$$

Recently, in Ref. [35] a PDF was introduced and defined by cumulants for arbitrary dimensions. Its special case $d=1$ corresponds to our cumulants in Eq. (15). There the χ^2 density with $2d$ degrees of freedom for large α was found, that for $d=1$ indeed gives Eq. (40).

IV. SCALING FUNCTION FOR WINDOW BOUNDARY CONDITION

A. Simulations

Although periodic $1/f^\alpha$ signals exist [1,32,33], most of the experimental signals displaying $1/f^\alpha$ spectrum are not periodic. Having a long experimental signal, however, the roughness can be calculated for small uncorrelated segments (these are called the windows) and the roughness distribution can be constructed for this ''window'' boundary condition, abbreviated as WBC. It is a plausible assumption that this PDF does not depend on the BCs of the original signal provided that the size of the window, T, is much smaller than the size of the entire signal T_p. Having uncorrelated windows would require large distances between them, however, in our experience the PDF remained unchanged even for overlapping windows. In the simulations of this chapter always nonoverlapping, but neighboring windows were used. Therefore it appears that the PDF of a Gaussian, perfect $1/f^\alpha$ signal with WBC can be computed having a long periodic signal of the same type. This method was applied numerically for general α and we report analytical results only for $\alpha=2$ and $\alpha=\infty$ in Sec. IV B.

The most accepted numerical way of generating a Gaussian $1/f^\alpha$ signal is to generate a Gaussian white noise first, filter the Fourier spectrum of it in order to get the desired $1/f^\alpha$ behavior (i.e., after a fast Fourier transformation its real and imaginary parts are multiplied by $f^{-\alpha/2}$), and finally transform it back. In this way the modes have amplitudes fluctuating around the desired $1/f^\alpha$ value, and have random phases. Calculating the roughness distribution of such periodic signals made it possible to check our theoretical predictions for periodic signals. The main advantage of generating periodic $1/f^\alpha$ signals is, however, that one can simulate WBC this way.

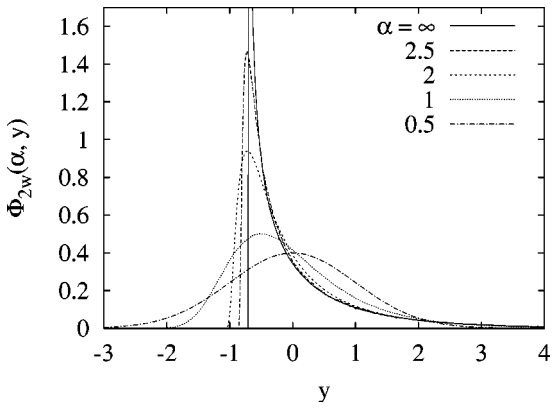

FIG. 4. Roughness distribution with WBC for different values of α as a function of the scaling variable (20). Note that the $\alpha=0.5$, 2, and ∞ curves are exact results.

Having the desired periodic signal of length T_p one can construct easily the PDF of the roughness of nonoverlapping parts of size T. The value of T_p was chosen to be at least 2^{20} while T varied between 2^6 and 2^{18}. The PDF converged to a size-independent shape for each values of α we have studied. The finite-size effect was larger for smaller values of α. For $\alpha=1$ the PDF for $T=2^6$ was already within a linewidth to the limit curve, however, for $\alpha=1/2$ such precision was only reached for $T=2^{18}$.

The results for a few values of alpha are depicted on Figs. 4 and 5 together with the two analytical results for WBC of Sec. IV B, which provided a good test for the numerics. One observes that the curves are changing continuously with alpha in the whole range of $[1/2,\infty]$. For $\alpha=1/2$ we recovered the Gaussian PBC result. It is also interesting to note that the $\alpha\to\infty$ convergence is noticeably faster than that in the PBC case. For WBC already the $\alpha=3$ PDF can be well approximated by that for $\alpha=\infty$.

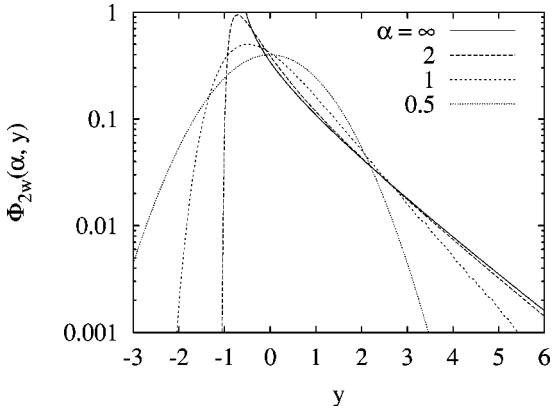

FIG. 5. The same as Fig. 4 but on log-linear scale.

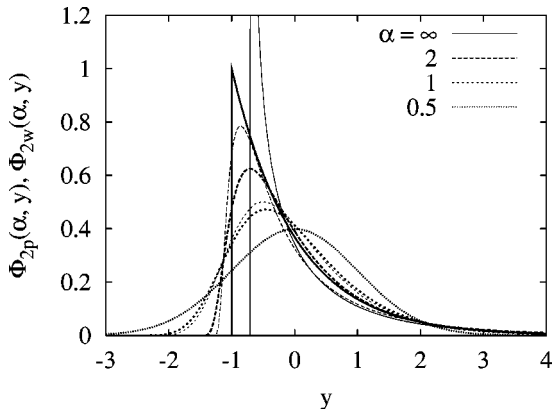

FIG. 6. Comparison of PBC (thick lines) and WBC (thin lines) for different values of α as a function of the scaling variable (20).

In Fig. 6 PDFs with different BCs are compared for several values of α. As we have already mentioned before, for $\alpha=1/2$ both BC result in a Gaussian PDF. For $\alpha=1$, as we already reported in Ref. [1], the difference between the PDFs are relatively small, namely, it was comparable to the precision of the experimental values. On Fig. 6 one can observe that the difference between the PDF with PBC and WBC are larger for larger values of α.

We should emphasize that the thresholds $\alpha=1$ and $\alpha=1/2$ were found to play the same role for PBC and WBC. Namely, the natural scaling of the roughness goes by the average and by the variance for $\alpha>1$ and $1>\alpha$, respectively, and for $\alpha\leqslant 1/2$ the scaled PDF becomes a Gaussian for both BCs. This evidence strongly supports our expectation that the scaling of cumulants for PBC, as summarized in Table I, also applies to WBC.

It is worth recalling that critical exponents in second-order phase transitions are generally believed not to depend on BC, but the scaling functions do vary below the upper critical dimension, the threshold for mean-field behavior, for different BCs [36,37,40]. The aforementioned BC independence of the scaling of the cumulants on the one hand, and the BC dependence of the scaled PDF for the roughness on the other one, show a close analogy with critical phenomena. The threshold for mean-field-type behavior is now $\alpha=1/2$, because below that the PDF is Gaussian.

B. Analytic results in special cases

1. Wiener process ($\alpha=2$)

Since the increments of the Wiener process are uncorrelated, the trajectory in a window is coupled to the path outside only by its two endpoints. However, if the length of the outer trajectory is much larger than that of the window then the endpoints appear essentially as unconstrained on the scale of the inner trajectory. Thus the WBC corresponds to the free BC in the $\alpha=2$ case. The generating function for free BC is, apart from scaling of s, the square root of the generating function for PBC as given below

$$G_{1w}(2,s)=\frac{\sqrt[4]{12s}}{\sqrt{\sinh\sqrt{12s}}}, \tag{41}$$

where the normalization $G_{1w}'(2,s)|_{s=0}=-1$ was used, corresponding to scaling by the average (19). This yields the PDF $\Phi_{1w}(2,x)$ by inverse Laplace transformation. Eq. (41) can be understood if one notes that free BC means that the action is diagonalized by cosine eigenfunctions, having zero derivatives at the endpoints. So the spectrum is labeled by integers, like for PBC, but there is no degeneracy. The generating function is in essence the reciprocal square-root determinant. While for PBC the square root disappears due to the twofold degeneracy, in free BC the root remains. A more rigorous derivation will be presented in [41].

The small-x series of the PDF $\Phi_{1w}(2,x)$ can be obtained by expanding Eq. (41) as

$$G_{1w}(2,s)=2\sqrt[4]{3s}\sum_{k=0}^{\infty}(-1)^k\binom{-1/2}{k}e^{-(4k+1)\sqrt{3s}}, \tag{42}$$

and using the Laplace transform of a single term in the sum as

$$\int_{c-i\infty}^{c+i\infty}\frac{ds}{2\pi i}e^{sx}\sqrt[4]{s}\,e^{-a\sqrt{s}}=\frac{a^{3/2}}{2\sqrt{2\pi}x^2}e^{-a^2/4x}\times {}_2F_0\left(-\frac{1}{4},-\frac{3}{4};-\frac{4x}{a^2}\right), \tag{43}$$

where ${}_2F_0$ is a hypergeometric function in standard notation [38]. Based on these relations we finally get

$$\begin{aligned}\Phi_{1w}(2,x)&=\int_{c-i\infty}^{c+i\infty}\frac{ds}{2\pi i}e^{sx}G_{1w}(2,s)\\&=\frac{3}{x^2\sqrt{2\pi}}\sum_{k=0}^{\infty}(4k+1)^{3/2}\frac{(2k-1)!!}{2^k k!}\\&\quad\times\exp\left(-\frac{3(4k+1)^2}{4x}\right)\\&\quad\times {}_2F_0\left(-\frac{1}{4},-\frac{3}{4};-\frac{4x}{3(4k+1)^2}\right).\end{aligned} \tag{44}$$

Although this can be considered as the small-x expansion, it is enough to retain the first three terms to get an estimation of $\Phi_{1w}(2,x)$ to a uniform precision of $\epsilon=6\times10^{-6}$ for any x. Similar to the PBC case, this is understood such that either the approximation deviates from the PDF by less than ϵ, or, the PDF is smaller than ϵ. To illustrate the accuracy of three terms from Eq. (44) for reasonable x-s, at $x=1$ they happen to give 53 digits of the PDF correctly. Series (44) has been used to draw the $\alpha=2$ curve of Figs. 4, 5, and 6.

2. Large α limit

As it has been discussed in Sec. III B 3, for large α only the lowest-frequency mode dominates the trajectory. In the full time interval with PBC, T_p, this means that

$$h(t)=r\cos\left(\frac{2\pi t}{T_p}+\varphi\right), \tag{45}$$

where $c_1=re^{i\varphi}/2$ is the Fourier coefficient of the $n=1$ mode. The fact that the real and imaginary parts of c_1 are independent, identically distributed, Gaussian variables has the consequence that the PDF for the polar parameters is

$$\rho(r,\varphi)=\frac{r}{2\pi a}e^{-r^2/2a}, \tag{46}$$

where we do not specify the variance a as it will disappear from the final formula anyhow.

Now we consider within the overall periodic signal $h(t)$ a small window of length $T\ll T_{\mathrm{p}}$. Since we shall average over the phase, we can take the window to be $[0,T]$. An expansion of Eq. (45) up to t^2 shows that the roughness of the trajectory within the window is in leading order

$$w_2=r^2b\sin^2\varphi, \tag{47}$$

where b is a constant depending on T and T_{p}, whose value will turn out to be immaterial. We thus have for the PDF of the roughness

$$P_{1\mathrm{w}}(\infty,w_2)=\int_0^\infty dr\int_0^{2\pi}d\varphi\,\rho(r,\varphi)\,\delta(w_2-r^2b\sin^2\varphi). \tag{48}$$

Inserting expression (46) for $\rho(r,\varphi)$ we get for the scaled variable $x=w_2/\langle w_2\rangle$ the PDF

$$\Phi_{1\mathrm{w}}(\infty,x)=\frac{e^{-x/2}}{\sqrt{2\pi x}}. \tag{49}$$

Note that, similar to the Wiener process, the large α limit of the generating function for the WBC is essentially the square root of that for PBC, apart from a scale change due to normalization. Indeed, the generating function for PBC is given by Eq. (39), while the Laplace transform for the above PDF is $(1+2s)^{-1/2}$.

V. $1/f^\alpha$ SURFACES IN ARBITRARY DIMENSIONS

So far we have considered random fields of one component that were functions of time, that is, a $1+1$-dimensional system. A natural generalization is to consider $d+1$-dimensional random surfaces, where the substrate has d-dimensional coordinates $\boldsymbol{x}$, and the field $h(\boldsymbol{x})$ still has one component. Imposing PBC now means that the substrate is a d-dimensional torus. Again, we define the probability density functional of a surface through an action that depends on the Fourier components $c_{\boldsymbol{n}}$ of the surface, $\boldsymbol{n}=(n_1,\ldots n_d)$, $n_j=-N,\ldots N$ being integers, and $c_{\boldsymbol{n}}=c^*_{-\boldsymbol{n}}$. The spatial unit is ℓ, the length of a period $L=N\ell$, the unit volume $v=\ell^d$, and the total d-dimensional volume $V=L^d$. (In the case of a usual surface $d=2$ and V is the area of the substrate.) The action is

$$S(\{c_{\boldsymbol{n}}\})=2\sigma V^{1-\alpha/d}{\sum_{\boldsymbol{n}}}'\,|\boldsymbol{n}|^\alpha|c_{\boldsymbol{n}}|^2. \tag{50}$$

Here prime means that the summation excludes the origin and counts only half of the remaining index space so that if a vector $\boldsymbol{n}$ is included then $-\boldsymbol{n}$ is not. For $\alpha=2$ this is the action associated with the stationary distribution of the Edwards-Wilkinson model [42]. In the case of general α-s, Eq. (50) is the long-range interaction part of the single-component version of the generalized $O(n)$ Hamiltonian of [43], for a recent reference see [44]. We shall briefly review some scaling properties for arbitrary dimensions in order to put $1/f^\alpha$ noise, as discussed in previous sections, in a broader perspective.

The roughness of a surface is a random variable, whose PDF can be derived similarly to the $d=1$ case discussed in Sec. II B. The short-range interaction case, $\alpha=2$, has been studied in detail by Refs. [24,25,34] for $d=2$ and by [45] for arbitrary dimension. The generating function of the PDF $P(w_2)$ is obtained as

$$G(s)=\prod_{\boldsymbol{n}}{}'\left(1+\frac{s}{\sigma V^{1-\alpha/d}|\boldsymbol{n}|^\alpha}\right)^{-1}, \tag{51}$$

whence the cumulants are

$$\kappa_k=\frac{(k-1)!}{(\sigma V^{1-\alpha/d})^k}{\sum_{\boldsymbol{n}}}'\,\frac{1}{|\boldsymbol{n}|^{\alpha k}}. \tag{52}$$

Note that the cumulants derived here were used to define the model of Ref. [35]. The sum converges for $\alpha k>d$, diverges logarithmically as $\ln N\propto\ln(V/v)$ for $\alpha k=d$ and like a power function as $N^{d-\alpha k}\propto(V/v)^{1-\alpha k/d}$ for $\alpha k<d$. The scaling properties of the cumulants are summarized in Table II.

For fixed d, in the large α limit, the modes with $|\boldsymbol{n}|=1$ dominate and so the roughness w_2 obeys the χ^2 distribution, as observed in Ref. [35]. For finite α, the threshold dimension where the mean logarithmically diverges is $d=\alpha$. For $d>\alpha$, however, $P(w_2)$ becomes a Dirac delta, but if one looks at it on the scale of the variance for large but finite N then a nontrivial function emerges for $d<2\alpha$. At $d=2\alpha$ the scale of the variance becomes larger than the scale of all higher cumulants, and thus for $d>2\alpha$ the scaling function is Gaussian. This represents normal finite-size scaling with fluctuations of the order of $V^{-1/2}$. Table II is in accordance with the known fact that $d=\alpha$ and $d=2\alpha$ can be viewed as the lower and upper critical dimension of the system, respectively [43].

It is reasonable to assume that the scaling of the cumulants as described above is not specific to the PBC used here, but generally characterizes $d+1$-dimensional Gaussian surfaces with dispersion exponent α for any BCs. Note that here only the scaling of averages were considered, the evaluation of distribution functions in arbitrary dimensions is beyond the scope of the present paper.

TABLE II. Scaling of the cumulants for various α-s for general dimension. The dots indicate that the last formula is valid from then on, i.e., " . . . " extends the validity to higher k-s and vertical dots to higher d-s.

Range or value of d	κ_1	$\sqrt{\kappa_2}$	$\sqrt[3]{\kappa_3}$	$\sqrt[4]{\kappa_4}$
$(0,\alpha)$	$V^{\alpha/d-1}$	$\cdots$		
α	$\ln\frac{V}{v}$	O(1)	$\cdots$	
$(\alpha,2\alpha)$	$v^{\alpha/d-1}$	$V^{\alpha/d-1}$	$\cdots$	
2α	$\vdots$	$V^{-1/2}\sqrt{\ln\frac{V}{v}}$	$V^{-1/2}$	$\cdots$
$(2\alpha,3\alpha)$		$v^{\alpha/d-1/2}\,V^{-1/2}$	$V^{\alpha/d-1}$	$\cdots$
3α		$\vdots$	$V^{-2/3}\sqrt[3]{\ln\frac{V}{v}}$	$V^{-2/3}$
$(3\alpha,4\alpha)$			$v^{\alpha/d-1/3}\,V^{-2/3}$	$V^{\alpha/d-1}$
			$\vdots$	

VI. FINAL REMARKS

As we have shown, the roughness distribution of periodic Gaussian $1/f^{\alpha}$ signals can be calculated for arbitrary α. The final expression is simple enough that it can be easily handled numerically and the scaling functions can be displayed in the relevant range of their argument. Also for WBC we provide a simple method to generate the scaling function by numerical simulation. Examining these scaling functions, we found an important feature in their α dependence. Namely, the shape of the functions varies noticeably with alpha in the physically rather interesting range of $1\leqslant\alpha\leqslant 2$. This observation underlies the usefulness and effectiveness of the roughness distribution as a tool for establishing common or distinct origins of scale-invariant behavior in different systems.

The present gallery of scaling functions is ready to be applied for determining accurate values of α in scale-invariant systems where the fluctuations are Gaussian. Since we have both the PBC and WBC scaling functions one can investigate models where PBC is used preferentially as well as experimental systems where WBC is usually obtained. Furthermore, the gallery can also be helpful in establishing the presence of non-Gaussian effects. It should be clear, however, the non-Gaussian effects are on the unfinished end of our study of roughness distributions. One can investigate the non-Gaussian effects in a given system by simulations [26,34] but the real question one should answer here is this: Can one find a classification of nonlinear theories which produce a given α, and can one find the roughness distributions for the various classes? Judging from the perspective of a related topic of critical dynamics this appears to be a highly nontrivial question.

ACKNOWLEDGMENTS

Thanks are due to L. B. Kish, Z. Gingl, and P. Holdsworth for illuminating discussions. This work was supported by the Hungarian Academy of Sciences (Grant No. OTKA T029792) and partly by the Swiss National Science Foundation.

[1] T. Antal, M. Droz, G. Györgyi, and Z. Rácz, Phys. Rev. Lett. **87**, 240601 (2001).
[2] C. Surya, ed., *Proceedings of the 15th International Conference on Noise in Physical Systems and* $1/f$ *Fluctuations* (IEEE Proceedings, Bentham Press, London, 1999).
[3] M.B. Weissman, Rev. Mod. Phys. **60**, 537 (1988).
[4] A.V. Yakimov and F.N. Hooge, Physica B **291**, 97 (2000).
[5] H.W. Press, Comments. Astrophys. **7**, 103 (1978).
[6] K.L. Schick and A.A. Verveen, Nature (London) **251**, 599 (1974).
[7] S. Mercik, K. Weron, and Z. Siwy, Phys. Rev. E **60**, 7343 (1999).
[8] F. Lillo and R.N. Mantegna, Phys. Rev. E **62**, 6126 (2000).
[9] B.B. Mandelbrot and J.R. Wallis, Water Resour. Res. **5**, 321 (1969).
[10] M. Yamamoto *et al.*, Brain Res. **366**, 279 (1986).
[11] D. Sornette, *Critical Phenomena in Natural Sciences* (Springer-Verlag, Berlin, 2000).
[12] K. Nagel and M. Paczuski, Phys. Rev. E **51**, 2909 (1995).
[13] X. Zhang and G. Hu, Phys. Rev. E **52**, 4664 (1995).
[14] P.H. Collins, M.S. Fuhrer, and A. Zetti, Appl. Phys. Lett. **76**, 894 (2000).
[15] L.B. Kiss *et al.*, Solid State Commun. **101**, 51 (1997).
[16] J. Krug and H. Spohn, in *Solids Far from Equilibrium*, edited by C. Godrèche (Cambridge University Press, Cambridge, England, 1991).
[17] U. Frisch, *Turbulence: The Legacy of A. N. Kolmogorov* (Cambridge University Press, Cambridge, England, 1995).
[18] P. Bak, C. Tang, and K. Wiesenfeld, Phys. Rev. Lett. **59**, 381 (1987).
[19] P. Bak, *How Nature Works* (Copernicus, New York, 1996).
[20] G. Korniss, Z. Toroczkai, M.A. Novotny, and P.A. Rikvold,

Phys. Rev. Lett. **84**, 1351 (2000).
[21] G. Tripathy and W. van Saarloos, Phys. Rev. Lett. **85**, 3556 (2000).
[22] S.T. Bramwell, P.C.W. Holdsworth, and J.-F. Pinton, Nature (London) **396**, 552 (1998).
[23] J.-F. Pinton, P.C.W. Holdsworth, and R. Labbé, Phys. Rev. E **60**, R2452 (1999).
[24] P. Archambault, S.T. Bramwell, and P.C.W. Holdsworth, J. Phys. A **30**, 8363 (1997).
[25] P. Archambault, S.T. Bramwell, J.-Y. Fortin, P.C.W. Holdsworth, S. Peysson, and J.-F. Pinton, J. Appl. Phys. **83**, 7234 (1998).
[26] E. Marinari, A. Pagnani, G. Parisi, and Z. Rácz, Phys. Rev. E **65**, 026136 (2002).
[27] E. J. Gumbel, *Statistics of Extremes* (Columbia University Press, New York, 1958).
[28] J. Galambos, *The Asymptotic Theory of Extreme Order Statistics* (R. E. Krieger, Malabar, Florida, 1987).
[29] K. Dahlstedt and H.J. Jensen, e-print cond-mat/0108007.
[30] D. Carpentier and P. LeDoussal, Phys. Rev. E **63**, 026110 (2001).
[31] S. Raychaudhuri, M. Cranston, C. Przybyla, and Y. Shapir, Phys. Rev. Lett. **87**, 136101 (2001).
[32] G. Foltin, K. Oerding, Z. Rácz, R.L. Workman, and R.K.P. Zia, Phys. Rev. E **50**, R639 (1994).
[33] M. Plischke, Z. Rácz, and R.K.P. Zia, Phys. Rev. E **50**, 3589 (1994).
[34] Z. Rácz and M. Plischke, Phys. Rev. E **50**, 3530 (1994).
[35] S.T. Bramwell, T. Fennel, P.C.W. Holdsworth, and B. Portelli, Europhys. Lett. **57**, 310 (2002).
[36] B. M. McCoy and T. T. Wu, *The Two Dimensional Ising Model* (Harvard University Press, Cambridge, MA, 1973).
[37] For exotic boundary conditions like Moebius strip and Klein bottle see K. Kaneda and Y. Okabe, Phys. Rev. Lett. **86**, 2134 (2001); W.T. Lu and F.Y. Wu, Phys. Rev. E **63**, 026107 (2001).
[38] M. Abramowitz and I. A. Stegun, *Handbook of Mathematical Functions*, 9th ed. (Dover, New York, 1964).
[39] We thank F. van Wijland for this observation.
[40] W.T. Lu and F.Y. Wu, Phys. Rev. E **63**, 026107 (2001).
[41] G. Györgyi and Z. Rácz (unpublished).
[42] T. Halpin-Healy and Y.-C. Zhang, Phys. Rep. **254**, 215 (1995).
[43] M.E. Fisher, S.-K. Ma, and B. Nickel, Phys. Rev. Lett. **29**, 917 (1972).
[44] H. Chamati, e-print cond-mat/0111449.
[45] S.T. Bramwell, J.-Y. Fortin, P.C.W. Holdsworth, S. Peysson, J.-F. Pinton, B. Portelli, and M. Sellitto, Phys. Rev. E **63**, 041106 (2001).
[46] S.T. Bramwell *et al.*, Phys. Rev. Lett. **84**, 3744 (2000).